

RESEARCH ARTICLE | MARCH 19 2024

# Introducing the concept of generalized thermal diffusivity to understand coupled heat–charge transport in ionic solutions

Special Collection: [Advances in Thermal Phonon Engineering and Thermal Management](#)

Antonio Cappai  ; Riccardo Dettori  ; Federica Marini  ; Claudio Melis   ; Luciano Colombo 

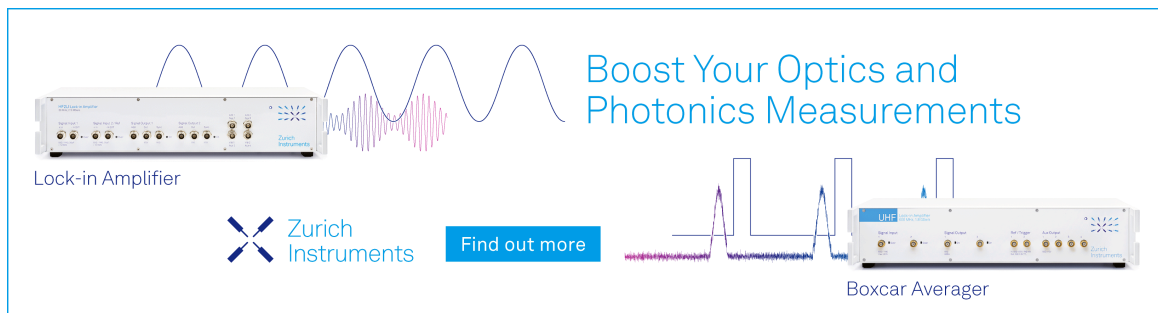


*Appl. Phys. Lett.* 124, 122203 (2024)

<https://doi.org/10.1063/5.0201444>



CrossMark



Boost Your Optics and Photonics Measurements

Lock-in Amplifier

Zurich Instruments

Find out more

Boxcar Averager

# Introducing the concept of generalized thermal diffusivity to understand coupled heat-charge transport in ionic solutions

Cite as: Appl. Phys. Lett. **124**, 122203 (2024); doi: 10.1063/5.0201444

Submitted: 30 January 2024 · Accepted: 6 March 2024 ·

Published Online: 19 March 2024



View Online



Export Citation



CrossMark

Antonio Cappai,  Riccardo Dettori,  Federica Marini,  Claudio Melis,<sup>a)</sup>  and Luciano Colombo 

## AFFILIATIONS

Department of Physics, University of Cagliari, Monserrato, Cagliari 09042, Italy

Note: This paper is part of the APL Special Collection on Advances in Thermal Phonon Engineering and Thermal Management.

<sup>a)</sup> Author to whom correspondence should be addressed: [claudio.melis@dsf.unica.it](mailto:claudio.melis@dsf.unica.it)

## ABSTRACT

A theoretical framework addressing the coupled thermal and charge transport phenomena in ionic solutions is here developed. Starting from the microscopic definitions of thermal and charge currents from Onsager formulation of non-equilibrium thermodynamics, a unique, very general and compact form of the governing differential equation for the evolution of a temperature profile is derived. In particular, the concept of generalized thermal diffusivity is introduced to capture the overall effect of the coupling between heat and charge transport in a single phenomenological coefficient as well as to shed light on the non-equivalent situations of concurrent or discordant heat and charge currents. To validate our theoretical framework, an ionic salt solution of NaCl in water is investigated.

© 2024 Author(s). All article content, except where otherwise noted, is licensed under a Creative Commons Attribution (CC BY) license (<http://creativecommons.org/licenses/by/4.0/>). <https://doi.org/10.1063/5.0201444>

In ionic systems, the simultaneous presence of electric fields and thermal gradients is a hallmark ruling over various physical phenomena and technological applications.<sup>1</sup> The emergence of temperature gradients in electrochemical devices, attributed to the Joule effect,<sup>2,3</sup> and the associated heat release during the corresponding chemical reactions<sup>4,5</sup> ultimately generate a net ionic current.<sup>6,7</sup> This electro-thermal coupling plays a key role in diverse technological domains, spanning nanoengines,<sup>8,9</sup> microfluidics,<sup>10,11</sup> and microbiology.<sup>12</sup> Additionally, ionic fluids are assuming a major role in various heat-transfer applications, such as waste-heat-recovery technologies,<sup>13</sup> solar energy storage,<sup>14</sup> and the design of molten salt reactors.<sup>15</sup> Improving our basic understanding of such subtle electro-thermal dynamics necessitates a quantitative mastery of the complex interplay between thermal and charge transport.

Recently, efforts in theoretical modeling of thermal transport in ionic fluids have been developed.<sup>16–18</sup> Thorough investigations on thermodiffusion effects and Soret phenomena have also been undertaken.<sup>6,19–22</sup> Furthermore, the exploration of ionic conductors as potential thermoelectric materials has gained prominence in recent years.<sup>6,23,24</sup> This interest arises from the limitations of traditional thermoelectric semiconductors, which, while demonstrating high performance at room temperature,<sup>25,26</sup> face practical constraints due to concerns related to their toxicity and rarity.<sup>27</sup>

Motivated by this state of affairs, we have developed the concept of generalized thermal diffusivity for a regime of coupled heat-charge transport. By blending together non-equilibrium thermodynamics and atomistic simulations, we make use of this parameter to shed light on the complex interplay between heat and charge carriers. Furthermore, the generalized thermal diffusivity is proved to be useful in describing the nonequivalent situations of concurrent (cg) or discordant (dg) thermal/electrostatic gradients. The implications of our findings extend beyond the specific system under investigation (a NaCl aqueous solution), providing a conceptual framework applicable to a broad spectrum of coupled heat-charge transport scenarios.

We will at first focus on the formal description of the very general case of a fluid binary system (sketched in Fig. 1) with a fixed volume  $\Omega$ . A total number of  $N$  charged particles are present and are free to move in an environment formed by  $N_0 \gg N$  neutral molecules. From a phenomenological standpoint, this is the formal representation of an ionic salt dissolved in a neutral solvent (e.g., NaCl in water). If the temperature  $T$  and the electrostatic potential  $V$  are not uniform across the sample (due to non-uniform temperature and ionic concentration profiles), heat  $\vec{J}_q$  and charge  $\vec{J}_c$  currents are present in the system. They are defined as:

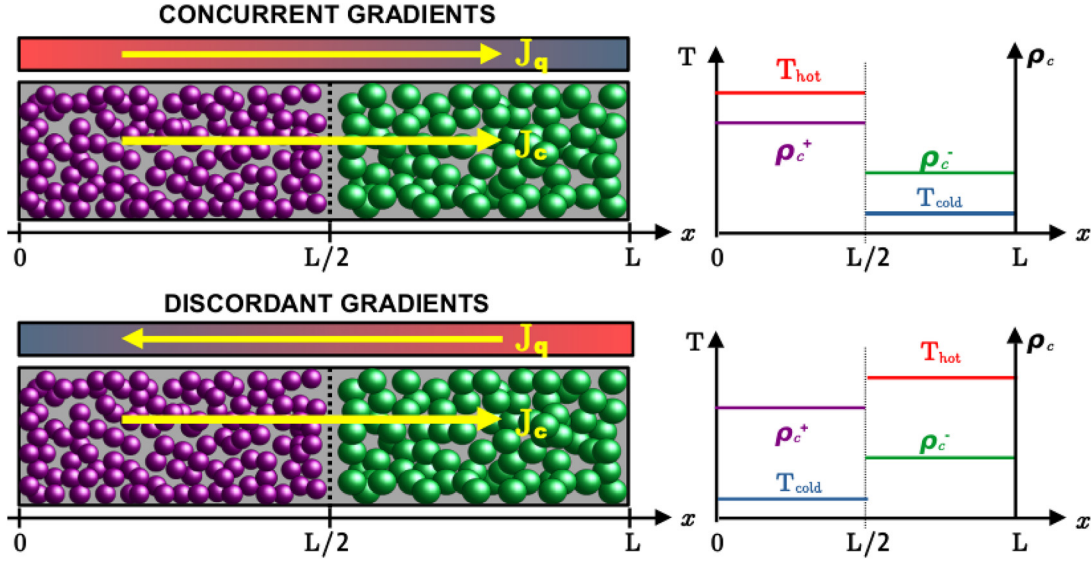


**FIG. 1.** Schematic representation of the initial configuration ( $t=0$ ) of the system analyzed. In the left panel, the arrangement of cations and anions (violet and green spheres, respectively) in the simulation cell with length  $L$  is shown, separated by a nominal interface (dashed line). The thermal bias initially imposed is rendered by color shadow, from red (hotter region) to blue (colder region), with heat  $J_q$  and charge  $J_c$  currents in yellow. In the right panel, the corresponding initial temperature and charge density profiles are represented: we will refer to the first case as the cg regime and to the second case as the dg regime.

$$\vec{J}_q = \frac{dQ}{dA dt} \hat{n}; \quad \vec{J}_c = \frac{dq}{dA dt} \hat{n}, \quad (1)$$

where  $dQ$  and  $dq$  are, respectively, the amount of heat and charge flowing in a time interval  $dt$  through a cross section  $dA$  normal to the unit vector  $\hat{n}$  (corresponding to the  $x$  direction in Fig. 1).

In general, heat and charge transport are not independent, as each particle carries both kinetic energy and charge. This is tantamount to state that both currents do depend on  $\vec{\nabla}T$  as well as  $\vec{\nabla}V$ . For this reason, a more general expression for both current vectors is needed in order to describe the evolution of the system. Non-equilibrium thermodynamics represents the natural theoretical framework to accomplish this task: starting from the hypothesis of a linear response regime, Onsager demonstrated that the generalized forces (namely  $\vec{\nabla}(1/T)$  and  $\vec{\nabla}V$ ) and the fluxes  $\vec{J}_q$  and  $\vec{J}_c$  are mutually linked by the system of differential equations<sup>28</sup>

$$\begin{cases} \vec{J}_q = L_{qq} \vec{\nabla} \left( \frac{1}{T} \right) + L_{qc} \left( -\frac{\vec{\nabla}V}{T} \right), \\ \vec{J}_c = L_{cq} \vec{\nabla} \left( \frac{1}{T} \right) + L_{cc} \left( -\frac{\vec{\nabla}V}{T} \right), \end{cases} \quad (2)$$

where  $L_{qq}$ ,  $L_{qc}$  =  $L_{cq}$ , and  $L_{cc}$  are referred to as *Onsager coefficients*; they are directly related to experimentally accessible quantities. If the system is kept at a constant and uniform temperature ( $\vec{\nabla}T = \vec{0}$ ), the isothermal electrical conductivity  $\sigma_0$  can be defined as

$$\sigma_0 \equiv \left( \frac{|\vec{J}_c|}{|\vec{\nabla}V|} \right)_{T_{\text{const}}} = \frac{L_{cc}}{T}. \quad (3)$$

Under the same conditions, a heat current is present due to the drift motion of the charge carriers (Peltier effect), and the ratio  $|\vec{J}_q|/|\vec{J}_c|$  defines the Peltier coefficient  $P$ ,

$$P \equiv \left( \frac{|\vec{J}_q|}{|\vec{J}_c|} \right)_{T_{\text{const}}} = \frac{L_{qc}}{\sigma_0 T}. \quad (4)$$

A pure thermal transport regime, instead, is defined by the condition  $\vec{J}_c = \vec{0}$ . The presence of  $P$  is, in this case, responsible for the onset of a  $\vec{\nabla}V \neq \vec{0}$ , and the thermal conductivity  $\kappa$  is thus written as

$$\kappa \equiv - \left( \frac{|\vec{J}_q|}{|\vec{\nabla}T|} \right)_{\vec{J}_c = \vec{0}} = \frac{1}{T^2} (L_{qq} - P^2 \sigma_0 T). \quad (5)$$

The use of phenomenological coefficients in Eqs. (3)–(5) allows to restate the expressions for the currents appearing in Eq. (2) in terms of experimentally accessible quantities,

$$\begin{cases} \vec{J}_q = - \left( \kappa + \frac{P^2 \sigma_0}{T} \right) \vec{\nabla}T - P \sigma_0 \vec{\nabla}V, \\ \vec{J}_c = - \frac{P \sigma_0}{T} \vec{\nabla}T - \sigma_0 \vec{\nabla}V, \end{cases} \quad (6)$$

which is indeed a noteworthy formulation that demonstrates the role of the Peltier coefficient as the key quantity in determining the heat-charge coupling. Interestingly enough, in the limit  $P \rightarrow 0$ , Eq. (6) simply reduces to Fourier's and Ohm's law, respectively.

If no sources or sinks of charge and heat exist in the system, two additional conditions must be satisfied, namely the conservation of thermal energy and charge. By introducing the concept of thermal energy density  $\rho_q = \mathcal{C}_v \rho_m T$ , where  $\mathcal{C}_v$  is the specific heat per unit mass,  $\rho_m$  the local mass density, and  $\rho_c$  the local charge density, the conservation laws can be expressed as

$$\frac{\partial \rho_q}{\partial t} + \vec{\nabla} \cdot \vec{J}_q = 0; \quad \frac{\partial \rho_c}{\partial t} + \vec{\nabla} \cdot \vec{J}_c = 0. \quad (7)$$

By imposing the constraints dictated by Eq. (7) in the expressions for the currents provided by Eq. (6), the time evolution of the temperature  $T$  can be straightforwardly derived. In the context of a linear response regime, it is found that

$$\frac{\partial T}{\partial t} = \frac{1}{\mathcal{E}_V \rho_m} \left[ \kappa + \frac{P^2}{T} \left( \frac{\sigma \sigma_0}{\sigma + \sigma_0} \right) \right] \nabla^2 T, \quad (8)$$

where  $\sigma$  is here introduced as

$$\sigma = \sigma_0 + \frac{P \sigma_0 |\nabla^2 T|}{T^2 |\nabla^2 V|}, \quad (9)$$

representing the electric conductivity evaluated when the temperature is not homogeneous; therefore, in the most general case,  $\sigma \neq \sigma_0$ . Equation (8) can be restated in a more compact form as

$$\frac{\partial T}{\partial t} = D_G \nabla^2 T, \quad (10)$$

where  $D_G$  denotes the *generalized thermal diffusivity*

$$D_G = \frac{1}{\mathcal{E}_V \rho_m} \left[ \kappa + \frac{P^2}{T} \left( \frac{\sigma \sigma_0}{\sigma + \sigma_0} \right) \right]. \quad (11)$$

This result clearly shows that the coupling between the thermal and charge currents is effectively described by a unique  $D_G$  coefficient, which, remarkably, can be separated in two terms,

$$D_G = \underbrace{\left[ \frac{\kappa}{\mathcal{E}_V \rho_m} \right]}_{\alpha_T} + \underbrace{\left[ \frac{1}{\mathcal{E}_V \rho_m} \frac{P^2}{T} \left( \frac{\sigma \sigma_0}{\sigma + \sigma_0} \right) \right]}_{D_{qc}}. \quad (12)$$

The first one is actually the ordinary thermal diffusivity observed when no charge transport occurs. The coupling term  $D_{qc}$  is expressed as a combination of material-specific parameters (namely, the isothermal and non-isothermal electric conductivities and the Peltier coefficient) and the temperature. It is noticeable that if the Peltier coefficient  $P$  is zero, the generalized thermal conductivity reduces to  $\alpha_T$ . The result is particularly important since  $D_G$  can be easily experimentally accessed; in fact, in our understanding, it is promptly linked to thermal conductivity measured in the coupled transport regime, while the usual  $\kappa$  is accessible [according to the definition in Eq. (5)] only when no charge current is flowing in the sample.

A paradigmatic case of unidimensional heat-charge coupled transport is conceptually represented in Fig. 1. Here, (left panels) the two nonequivalent cg and dg situations addressed below are schematically shown. By setting a step-like temperature and charge density profile at  $t=0$ , the time-evolution of the spatially averaged temperature difference  $\langle \Delta T(t) \rangle$  between the two regions of the system is given by

$$\langle \Delta T(t) \rangle = \frac{8\Delta T(0)}{\pi^2} \left[ \sum_{m=0}^{\infty} \frac{1}{a(m)^2} \exp \left( -\frac{4\pi^2 a(m)^2}{L^2} D_G t \right) \right], \quad (13)$$

where  $\Delta T(0)$  denotes the initial temperature difference, and  $a(m) = 2m + 1$ .

To assess the validity of the above-mentioned formal results, we performed a classical molecular dynamics simulation of an aqueous NaCl electrolyte solution. Simulations were performed using

LAMMPS<sup>29</sup> package with a q-TIP4P/F<sup>30</sup> force field. This interaction scheme was parameterized to provide an accurate description of the liquid structure, diffusion coefficient, and infrared absorption frequencies of water as well as its anomalous density behavior including the correct density maximum and melting temperature. Sodium (Na) and chlorine (Cl) ions were modeled according to the scaled-ionic-charge model by Kann and Skinner for ions.<sup>31</sup> Water molecules were held rigid using the SHAKE algorithm,<sup>32</sup> and we adopted a cutoff radius of 12.0 Å for Lennard-Jones interactions, while Coulombic interactions were computed adopting a particle-particle-particle-mesh solver adapted for the TIP4P water force-field with a  $10^{-5}$  accuracy. We initially set up a  $50.09 \times 50.09 \times 200.36$  Å<sup>3</sup> simulation box containing 16704 water molecules at a fixed density of 0.994 g/cm<sup>3</sup>, which was initially optimized and equilibrated at  $T = 300$  K for 50 ps using a canonical sampling velocity rescaling thermostat.<sup>33</sup> We then realized the electrolyte solution at eight different concentrations, namely 0.035, 0.07, 0.085, 0.165, 0.170, 0.275, 0.33 M, and 0.55 M. To explore heat-charge coupled transport phenomena, we initially generated a charge gradient within the simulation cell by placing all Na<sup>+</sup> ions in the left half region of the box and the Cl<sup>-</sup> ions in the opposite half. Then, a step-like temperature gradient was imposed by thermostating one half of the cell at  $T_{\text{hot}} = 325$  K and the other at  $T_{\text{cold}} = 275$  K over a duration of 4 ps. The system was next aged in the microcanonical ensemble for a total of 50 ps. Due to the concentrations considered in this work, which were chosen to be comparable with typical concentrations of aqueous electrolytes,<sup>34–37</sup> the number of anions and cations is very small compared to the number of water molecules: to improve the statistical significance of our simulations, we therefore performed configurational average over 25 independent replicas, in which we assigned different initial velocities and different initial positions to ionic species. Furthermore, to investigate possible size effects, calculations were repeated, with fixed solute concentration, also with simulation cells with  $L_x = 100$  Å and  $L_x = 300$  Å, the number of solvent molecules consistently scaled to keep the overall mass density of the  $L_x = 200$  Å case. We found that  $D_G$  slightly depends on the size of the system: by evaluating the parameter at 100, 200, and 300 Å, in cg regime, we calculated  $D_G$  as large as 18.0, 20.2, and  $21.3 \times 10^{-8}$  m<sup>2</sup>/s, respectively. Since convergence is substantially achieved at  $L = 200$  Å, we consistently carried the following analysis at this length.

The results of atomistic simulations conducted on a 200 Å-long sample are shown in Fig. 2. The time evolution of the average temperature difference  $\langle \Delta T(t) \rangle$  between the right and left regions is presented for two cases of interest: in the completely realistic scenario where the two chemical species in the solvent are charged (red line) and in the case where the two species are neutral (green line). In the latter case, where the ionic charges are arbitrarily set to zero, the simulation was carried out to study the system in a purely thermal regime.

In both cases, we observe that the evolution of the temperature difference, as predicted by Eq. (13), is substantially obeyed by the simulation. We therefore conclude that the theoretical framework here adopted, based on the assumption of a linear response [see Eq. (2)] is sufficient to model the coupled heat-charge transport regime.

Figure 2 reveals a coupling effect between heat and charge transport, as shown by the different time evolution of  $\langle \Delta T(t) \rangle$  in the case of a charged solvent compared to its neutral counterpart. It is emphasized that the initial temperature gradient appears to dampen more rapidly in the case of an electrically neutral solvent, a difference quantitatively

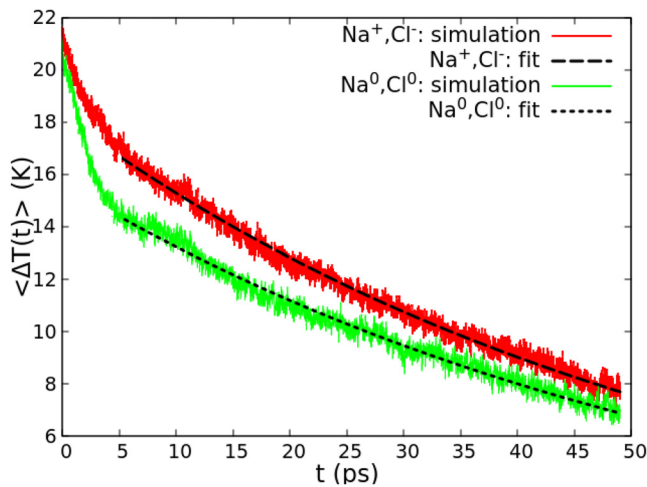


**FIG. 2.** Time evolution of  $\langle \Delta T(t) \rangle$  [see Eq. (13)] during a microcanonical run in the case of a system with  $L_x = 200$  Å. Initial temperature difference is set in cg (as defined in Fig. 1) both for charged ( $\text{Na}^+, \text{Cl}^-$ ) and neutral ( $\text{Na}^0, \text{Cl}^0$ ) solute configurations (red and green line, respectively). Results of fitting procedure using Eq. (13) are shown as dashed black lines.

measured by fitting the time series using the analytical solution in Eq. (13). We remark that while in the charged case the fitting parameter  $D_G$  represents the generalized thermal diffusivity as defined in Eq. (11), and in the case of a neutral solvent, it should be understood as the sole thermal diffusivity.

The fitting of the calculated  $\langle \Delta T(t) \rangle$  by Eq. (13) is shown in Fig. 2 (black lines), with the fitting region restricted to the interval  $t \geq 5$  ps, implying that the  $\Delta T(0)$  term appearing in Eq. (13) is actually evaluated at  $t = 5$  ps. This limitation arises from the presence of some fictitious nonlinear effects observed during the initial phases of the microcanonical simulation, a phenomenon extensively discussed.<sup>38–42</sup> Given that these deviations from linearity quickly dissipate without affecting the overall validity of the results, as customary, we have excluded these initial stages from the fitting procedure.

Repeating the analysis for different solute molar concentrations (both in the charged and neutral cases) highlighted a substantially monotonic trend of  $D_G$  as a function of concentration, as shown in Fig. 3. The most interesting result emerged, however, from the comparison with the inversion of the initial temperature profile at constant charge distribution and solute concentration. Compared to the data presented in Fig. 3 in the cg and dg regime, a sizeable difference in the evolution trend of  $D_G$  as a function of concentration is clearly found: while in cg,  $D_G$  appears to monotonically decrease with concentration, in the dg case, a clear increasing trend is observed. In other words, for sufficiently high molar concentrations, the system exhibits unlike behaviors for the dg and cg regimes. We will hereafter refer to this feature as a rectification behavior of thermal current.

The origin of this rectification effect is challenging and deserves a more careful analysis. We identify two possible causes, not mutually exclusive, that may be at its origin, namely (i) the different mass of the two chemical species forming the solute and (ii) the specific effect of charge–heat coupling. In this perspective, the possibility to exactly

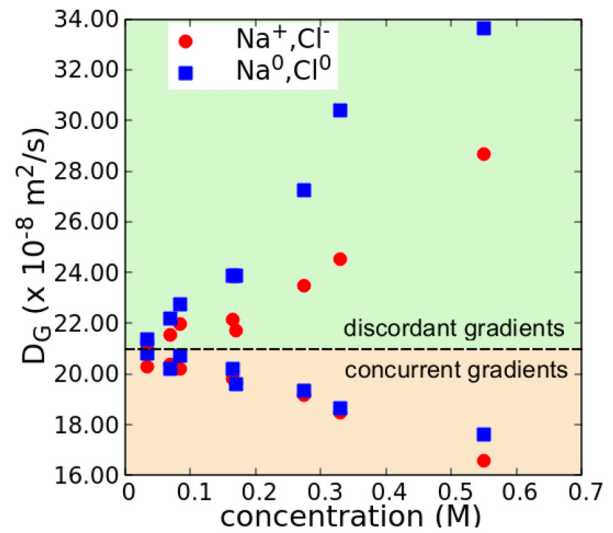


**FIG. 3.** Generalized thermal diffusivity  $D_G$  as a function of molar concentration of solute for the paradigmatic case of a sample with  $L_x = 200$  Å.  $D_G$  values are calculated for both charged and neutral solute, respectively, labeled as ( $\text{Na}^+, \text{Cl}^-$ ) and ( $\text{Na}^0, \text{Cl}^0$ ) and for cg and dg (as defined in Fig. 1).

decouple  $D_G$  in a pure thermal component and a coupling term [see Eq. (12)] is very useful, allowing a quantitative estimate of cause (ii).

In order to demonstrate the presence and quantify the extent of cause (i), we observe that rectification persists both when the system is in a coupled transport regime and in the case of pure thermal transport. Addressing the case of a neutral solute, the presence of a thermal diffusivity dependent on the applied initial temperature profile suggests that rectification is mainly due to a Soret effect. This result is reasonable, considering that the two analyzed chemical species have sizably different atomic masses ( $M_{\text{Na}}/M_{\text{Cl}} = 0.65$ ). We thus attribute the difference between the generalized thermal diffusivity in cg and dg ( $D_G^{\text{cg}}$  and  $D_G^{\text{dg}}$ , respectively) observed in the case of a neutral solute as a consequence of Soret effect.

A comparison of the neutral and charged case (see Fig. 3) allows us to observe that a charge–heat coupling is also present. Indeed, especially at high concentrations, it emerges that the generalized thermal diffusivity in the case of a charged solute deviates from the corresponding value for a neutral solute. To better highlight this deviation, the contribution of  $D_{qc}$  was quantified, as shown in the left panel of Fig. 4 for both the cg and dg regime. We observe preliminarily that in absolute terms,  $D_{qc}$  can reach values as large as 13% of  $D_G$ . For this reason, the system, even if dominated by a purely thermal transport regime, exhibits a significant heat–charge coupling effect. We interpret such a sizeable contribution as a consequence of the large internal electric field, which we estimate to be  $\sim 10^6$  V/m. A second interesting result emerges by observing the variation of  $D_{qc}$  with the solute concentration, which exhibits an opposite trend compared to  $D_G$ . In fact,  $D_{qc}$  clearly monotonically decreases with solute concentration in the dg, while an overall increase is found in cg. Moreover, the magnitude of the variation with solute concentration is more prominent in the dg, with  $|D_{qc}|$  spanning from  $|D_{qc}| \simeq 0$  up to  $6.00 \times 10^{-8} \text{ m}^2/\text{s}$ . In cg, instead,  $|D_{qc}|$  is less sensitive than the solute concentration.



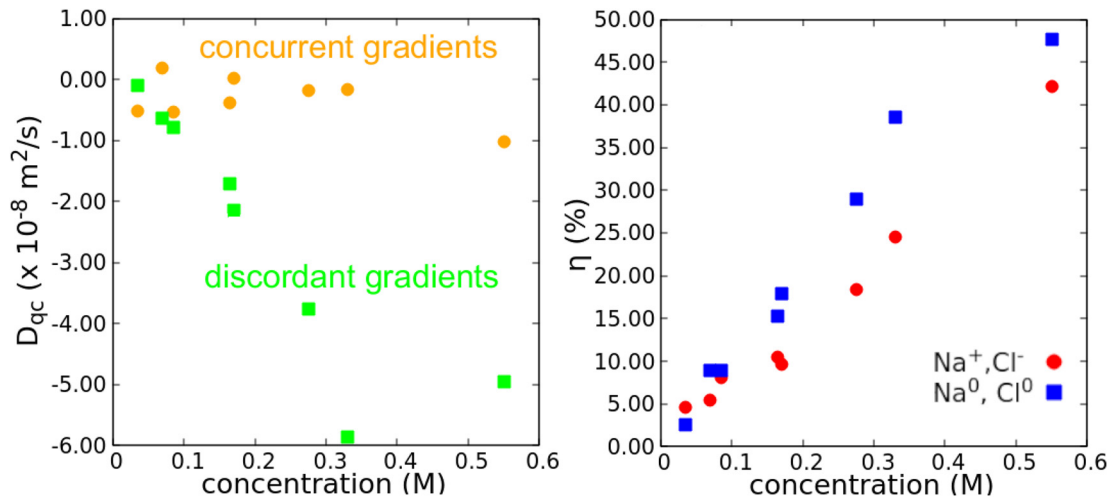


**FIG. 4.** Left: coupling diffusivity  $D_{gc}$  [as implicitly defined by Eq. (12)] in cg and dg as a function of the molar concentration of solute. Right: rectification parameter  $\eta$  [defined in Eq. (14)] as a function of the molar concentration of solute, in charged and neutral case, labeled as  $(\text{Na}^+, \text{Cl}^-)$  and  $(\text{Na}^0, \text{Cl}^0)$ , respectively.

To conclude the characterization of rectification properties of the system, we introduce a dimensionless coefficient  $\eta$  to quantify the size of the rectification. More specifically, we define  $\eta$  as the relative difference between generalized thermal diffusivity in the cg and dg regimes as

$$\eta = \frac{|D_G^{cg} - D_G^{dg}|}{D_G^{cg}} \cdot 100. \quad (14)$$

Consistent with the observed trend in Fig. 3,  $\eta$  appears to monotonically increase with solute concentration, as shown in the right panel of Fig. 4, reaching values as large as  $\sim 45\%$ .

It can thus be concluded that the principal origin of the rectification is mainly due to a Soret effect. We also remark the presence of a dramatic reduction of the generalized thermal conductivity in the case of charged solute compared to the corresponding neutral case. We attribute this decrease to the

modification of the arrangement of water molecules, since it has been demonstrated in the literature<sup>42,43</sup> that the intricate network of the hydrogen bond is crucial in determining the thermal transport. In order to definitely elucidate this phenomenon, oxygen–oxygen and oxygen–hydrogen radial distribution function [ $g_{\text{OO}}(r)$  and  $g_{\text{OH}}(r)$ , respectively] are represented in Fig. 5.  $g(r)$  functions were calculated for pure water (black line) and in the case of a charged (red) and neutral (blue) 0.55M solution. The results show that while the addition of a neutral solute only marginally affects the position and width of the radial distribution functions, large modifications are found if the solute is charged. In particular, the broadening of the peaks in  $g(r)$  indicates a more random distribution in the first solvation shell, while second and third peaks are almost suppressed, indicating a sizeable modification of the microscopic hydrogen bonding network. In our understanding, this disruption is responsible for the dramatic decrease in  $D_G$ , since

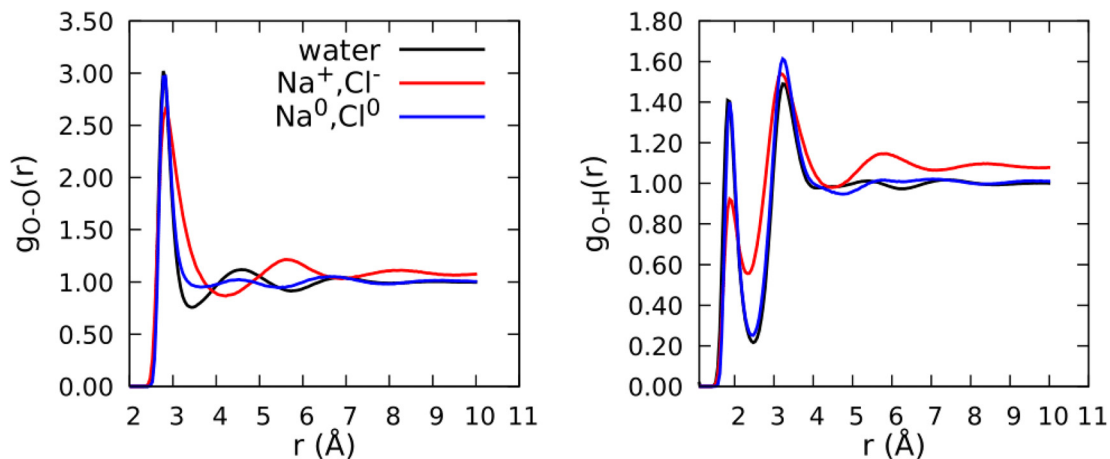


**FIG. 5.** Oxygen–oxygen radial distribution function  $g_{\text{OO}}(r)$  (left) and oxygen–hydrogen  $g_{\text{OH}}(r)$  calculated for pure water (black line) and in the case of a charged (red) and neutral (blue) 0.55M solution.

hydrogen bonds-mediated vibrations play a significant role in determining the overall heat transport in water. This, in turn, decreases also the entity of  $\eta$  rectification parameter.

In conclusion, we have worked out the concept of “generalized thermal conductivity,” which embodies the subtle entanglement between thermal and electrical currents and enables the understanding of the two nonequivalent regimes of concurrent or discordant heat-charge fluxes. We found that a rectification behavior emerges, and by analyzing the pure thermal and coupled terms of  $D_G$ , we were able to identify the exact role of Soret-like thermal transport as well as the alteration of water microstructure as the main source of the peculiar thermal response of the system.

The authors acknowledge the financial support under the National Recovery and Resilience Plan (NRRP; Mission 4, Component 2, Investment 1.3—Call for tender No. 341 published on March 13, 2022) by the Italian Ministry of University and Research (MUR), funded by the European Union—NextGenerationEU (No. PE00000021), Concession Decree No. 1561, adopted on October 11, 2022 by MUR, CUP F53C22000770007, through the project titled “NEST—Network 4 Energy Sustainable Transition.” We acknowledge the CINECA award, under the ISCRA initiative, for the availability of high-performance computing resources and support.

## AUTHOR DECLARATIONS

### Conflict of Interest

The authors have no conflicts to disclose.

### Author Contributions

**Antonio Cappai:** Conceptualization (equal); Data curation (lead); Formal analysis (lead); Methodology (lead); Visualization (lead); Writing – original draft (lead); Writing – review & editing (lead). **Riccardo Dettori:** Data curation (lead); Formal analysis (equal); Methodology (lead); Software (lead); Writing – original draft (equal); Writing – review & editing (equal). **Federica Marini:** Formal analysis (equal). **Claudio Melis:** Conceptualization (equal); Funding acquisition (equal); Supervision (equal); Writing – original draft (equal); Writing – review & editing (equal). **Luciano Colombo:** Conceptualization (equal); Supervision (equal); Writing – original draft (equal); Writing – review & editing (equal).

### DATA AVAILABILITY

The data that support the findings of this study are available from the corresponding author upon reasonable request.

## REFERENCES

- A. Grisafi and F. Grasselli, “Effect of a temperature gradient on the screening properties of ionic fluids,” *Phys. Rev. Mater.* **7**, 045803 (2023).
- J. A. Wood, A. M. Benneker, and R. G. Lammertink, “Temperature effects on the electrohydrodynamic and electrokinetic behaviour of ion-selective nanochannels,” *J. Phys.: Condens. Matter* **28**, 114002 (2016).
- L. Shi, Z. Han, Y. Feng, C. Zhang, Q. Zhang, H. Zhu, and S. Zhu, “Joule heating of ionic conductors using zero-phase frequency alternating current to suppress electrochemical reactions,” *Engineering* **25**, 138–143 (2023).
- M. E. Van Valkenburg, R. L. Vaughn, M. Williams, and J. S. Wilkes, “Thermochemistry of ionic liquid heat-transfer fluids,” *Thermochim. Acta* **425**, 181–188 (2005).
- J. Guillaumon, C. Love, R. Carter, X. Yang, and A. Verma, “Electrolyte conditions in lithium-ion batteries in presence of a thermal gradient,” *MRS Adv.* **6**, 564–569 (2021).
- L. Fu, L. Joly, and S. Merabia, “Giant thermoelectric response of nanofluidic systems driven by water excess enthalpy,” *Phys. Rev. Lett.* **123**, 138001 (2019).
- M. T. Børset, X. Kang, O. S. Burheim, G. M. Haarberg, Q. Xu, and S. Kjelstrup, “Seebeck coefficients of cells with lithium carbonate and gas electrodes,” *Electrochim. Acta* **182**, 699–706 (2015).
- B. Szukiewicz, U. Eckern, and K. I. Wysokiński, “Optimisation of a three-terminal nonlinear heat nano-engine,” *New J. Phys.* **18**, 023050 (2016).
- H. Ding, P. S. Kollipara, Y. Kim, A. Kotnala, J. Li, Z. Chen, and Y. Zheng, “Universal optothermal micro/nanoscale rotors,” *Sci. Adv.* **8**, eabn8498 (2022).
- A. Salari, M. Navi, T. Lijnse, and C. Dalton, “Ac electrothermal effect in microfluidics: A review,” *Micromachines* **10**, 762 (2019).
- S. Liu, L. Lin, and H.-B. Sun, “Opto-thermophoretic manipulation,” *ACS Nano* **15**, 5925–5943 (2021).
- C. Liu, J. Zhao, F. Tian, L. Cai, W. Zhang, Q. Feng, J. Chang, F. Wan, Y. Yang, B. Dai *et al.*, “Low-cost thermophoretic profiling of extracellular-vesicle surface proteins for the early detection and classification of cancers,” *Nat. Biomed. Eng.* **3**, 183–193 (2019).
- S. Kjelstrup, K. R. Kristiansen, A. F. Gunnarshaug, and D. Bedeaux, “Seebeck, Peltier, and Soret effects: On different formalisms for transport equations in thermogalvanic cells,” *J. Chem. Phys.* **158**(2), 020901 (2023).
- A. A. Minea, “Overview of ionic liquids as candidates for new heat transfer fluids,” *Int. J. Thermophys.* **41**, 151 (2020).
- Y. Wang, C. Zeng, and W. Li, “The influence of temperature gradient on the corrosion of materials in molten fluorides,” *Corrosion Sci.* **136**, 180–187 (2018).
- N. Ohtori, M. Salanne, and P. A. Madden, “Calculations of the thermal conductivities of ionic materials by simulation with polarizable interaction potentials,” *J. Chem. Phys.* **130**(10), 104507 (2009).
- R. Bertossa, F. Grasselli, L. Ercole, and S. Baroni, “Theory and numerical simulation of heat transport in multicomponent systems,” *Phys. Rev. Lett.* **122**, 255901 (2019).
- F. Grasselli and S. Baroni, “Invariance principles in the theory and computation of transport coefficients,” *Eur. Phys. J. B* **94**, 160 (2021).
- N. E. Zimmermann, G. Guevara-Carrion, J. Vrabec, and N. Hansen, “Predicting and rationalizing the Soret coefficient of binary Lennard-Jones mixtures in the liquid state,” *Adv. Theory Simul.* **5**, 2200311 (2022).
- S. Bonella, M. Ferrario, and G. Ciccotti, “Thermal diffusion in binary mixtures: Transient behavior and transport coefficients from equilibrium and nonequilibrium molecular dynamics,” *Langmuir* **33**, 11281–11290 (2017).
- J. E. Vos, D. I. Maur, H. P. Rodenburg, L. Van den Hoven, S. E. Schoemaker, P. E. de Jongh, and B. H. Ern e, “Electric potential of ions in electrode micropores deduced from calorimetry,” *Phys. Rev. Lett.* **129**, 186001 (2022).
- A. Cappai, L. Colombo, and C. Melis, “Modeling the coupled mass-heat transport in Lennard-Jones-like binary mixtures by approach-to-equilibrium molecular dynamics,” *Adv. Theory Simul.* 2300849 (published online, 2024).
- B. Huang, M. Roger, M. Bonetti, T. Salez, C. Wiertel-Gasquet, E. Dubois, R. Cabreira Gomes, G. Demouchy, G. M eriguet, V. Peyre *et al.*, “Thermoelectricity and thermodiffusion in charged colloids,” *J. Chem. Phys.* **143**(5), 054902 (2015).
- T. Li, X. Zhang, S. D. Lacey, R. Mi, X. Zhao, F. Jiang, J. Song, Z. Liu, G. Chen, J. Dai *et al.*, “Cellulose ionic conductors with high differential thermal voltage for low-grade heat harvesting,” *Nat. Mater.* **18**, 608–613 (2019).
- C. Gayner and K. K. Kar, “Recent advances in thermoelectric materials,” *Prog. Mater. Sci.* **83**, 330–382 (2016).
- C. Artini, G. Pennelli, P. Graziosi, Z. Li, N. Neophytou, C. Melis, L. Colombo, E. Isotta, K. Lohani, P. Scardi *et al.*, “Roadmap on thermoelectricity,” *Nanotechnology* **34**, 292001 (2023).
- V. M. Barrag n, K. R. Kristiansen, and S. Kjelstrup, “Perspectives on thermoelectric energy conversion in ion-exchange membranes,” *Entropy* **20**, 905 (2018).
- S. Kjelstrup and D. Bedeaux, *Non-Equilibrium Thermodynamics of Heterogeneous Systems*, Series on Advances in Statistical Mechanics, 2nd ed. (World Scientific Publishing Company, 2020).
- S. Plimpton, “Fast parallel algorithms for short-range molecular dynamics,” *J. Comput. Phys.* **117**, 1–19 (1995).

- <sup>30</sup>S. Habershon, T. E. Markland, and D. E. Manolopoulos, "Competing quantum effects in the dynamics of a flexible water model," *J. Chem. Phys.* **131**, 024501 (2009).
- <sup>31</sup>Z. R. Kann and J. L. Skinner, "A scaled-ionic-charge simulation model that reproduces enhanced and suppressed water diffusion in aqueous salt solutions," *J. Chem. Phys.* **141**, 104507 (2014).
- <sup>32</sup>H. C. Andersen, "Rattle: A "velocity" version of the shake algorithm for molecular dynamics calculations," *J. Comput. Phys.* **52**, 24–34 (1983).
- <sup>33</sup>G. Bussi, D. Donadio, and M. Parrinello, "Canonical sampling through velocity rescaling," *J. Chem. Phys.* **126**, 014101 (2007).
- <sup>34</sup>K. J. Muller and H. G. Hertz, "A parameter as an indicator for water-water association in solutions of strong electrolytes," *J. Phys. Chem.* **100**, 1256–1265 (1996).
- <sup>35</sup>R. Lipowsky, W. Konings, E. Sackmann, H. Kaback, and J. Lolkema, *Handbook of Biological Physics* (Elsevier, 1995), Vol. 1, pp. 603–642.
- <sup>36</sup>J. Lyklema, *Fundamentals of Interface and Colloid Science. Volume 2: Solid-Liquid Interfaces. With Special Contributions by A. de Keizer, B.H. Bijsterbosch, G.J. Fleer and M.A. Cohen Stuart.* (Academic Press, 1995).
- <sup>37</sup>J. Israelachvili, *Intermolecular and Surface Forces* (Elsevier Science, 2010).
- <sup>38</sup>E. Lampin, P. L. Palla, P.-A. Francioso, and F. Cleri, "Thermal conductivity from approach-to-equilibrium molecular dynamics," *J. Appl. Phys.* **114**, 033525 (2013).
- <sup>39</sup>C. Melis, R. Dettori, S. Vandermeulen, and L. Colombo, "Calculating thermal conductivity in a transient conduction regime: Theory and implementation," *Eur. Phys. J. B* **87**, 96 (2014).
- <sup>40</sup>C. Cattaneo, "Sur une forme de l'equation de la chaleur eliminant la paradoxe d'une propagation instantanee," *C. R. Acad. Sci.* **247**, 431–433 (1958).
- <sup>41</sup>D. D. Joseph and L. Preziosi, "Heat waves," *Rev. Mod. Phys.* **61**, 41–73 (1989).
- <sup>42</sup>R. Dettori, M. Ceriotti, J. Hunger, C. Melis, L. Colombo, and D. Donadio, "Simulating energy relaxation in pump-probe vibrational spectroscopy of hydrogen-bonded liquids," *J. Chem. Theory Comput.* **13**, 1284–1292 (2017).
- <sup>43</sup>R. Dettori, M. Ceriotti, J. Hunger, L. Colombo, and D. Donadio, "Energy relaxation and thermal diffusion in infrared pump-probe spectroscopy of hydrogen-bonded liquids," *J. Phys. Chem. Lett.* **10**, 3447–3452 (2019).